

A numerical study on the optimization of an airfoil design

Yiding Feng

School of Mechanical Engineering, The University of Adelaide, Adelaide, Australia

2116848598@qq.com

Abstract. How to optimize the design of an airfoil to achieve excellent aerodynamic performance has always been a popular research topic, because the wing is the main source of the lift of an airplane. Improving the lift-to-drag ratio (L/D ratio) is often taken as the aim for airfoil design optimization. In the optimization process, it is required to optimize one of the shape parameters of the airfoil under the premise of keeping the rest of the shape parameters consistent till the optimal L/D ratio is reached. This paper studies how the camber affects the L/D ratio of an airfoil using the CFD method and optimizes the airfoil design based on the camber. Three airfoils with different camber were simulated in 2D using the software COMSOL. The graphs of the L/D ratio at different angles of attack (AOA) for these three airfoils were plotted, and the results reveal that the airfoil with the highest camber has the optimal L/D ratio. Therefore, high camber is a good choice to improve the L/D ratio of an airfoil in airfoil design.

Keywords: airfoil; computational fluid dynamics; optimization; lift-to-drag ratio.

1. Introduction

The wing of the airplane produces lift and drag in flight, and most of the lift of an airplane is provided by the wing. The ratio between lift and drag generated by an airfoil is called the lift-to-drag ratio (L/D ratio). The L/D ratio is one of the most important aerodynamic performance parameters in designing airfoils as a high L/D ratio indicates the airplane can glide farther at a given altitude, carry a larger payload and fly longer in the sky [1]. Therefore, optimizing the airfoil design to achieve the optimal L/D ratio is necessary. Besides, the L/D ratio varies with the angle of attack (AOA) and reaches the maximum at a certain AOA. Flying at the AOA that yields the highest L/D ratio provides a high flight efficiency to the airplane [2]. Many researchers have already attempted to optimize the airfoil design with different methods. Acarer [3] studied the effect of passive leading-edge slots in the L/D ratio using the DU12W262 airfoil and found out that the airfoils with slots have higher peak and overall L/D ratio than the conventional airfoils. Sogukpinar and Bozkurt [4] conducted an airflow simulation for the NACA 63₂-215 airfoil at different AOA using the SST turbulence model, and they found that the L/D ratio increases at the AOA from 0° to 4°, after reaching the maximum around the AOA of 4°, the L/D ratio starts to decrease, thus the optimal AOA for NACA 63₂-215 airfoil is approximately 4°. Hong et al [5] selected NACA 4412, NACA 0009 and NACA 23012 airfoils for the wind tunnel blade analysis, and it was found that the L/D ratio is higher than that of NACA 0009 and NACA 23012 in the range of $-5^\circ \leq \text{AOA} \leq 9^\circ$, after the AOA exceeds 9°, and L/D ratio of NACA 23012 is the highest among these three airfoils. Haryanto et al [6] applied Genetic Algorithm (GA) to shape optimization of an airfoil and obtained the optimal airfoil shape which has the maximum L/D ratio, and compared it with the results

obtained from the based-gradient method, they found that the optimization results obtained from GA are better than that obtained from the based-gradient method, because the airfoil shape optimized by the based-gradient method has a maximum L/D ratio of 29.96, whereas the maximum L/D ratio of the airfoil shape optimized by GA is 31.101. Zhang et al [7] applied the CSA-KJ method to optimize the shape of NACA 4412 airfoil and obtained the CSA-KJ4412 airfoil, the overall L/D ratio of CSA-KJ4412 airfoil is 4.53% higher than that of NACA 4412 airfoil. He, Agarwal and Ganguli [8] applied the multiobjective genetic algorithm (MOGA) to the shape optimization of the wind turbine airfoil S809 and simulated the airflow field around the airfoil using the software FLUENT, and the results showed that the L/D ratio of the optimized S809 airfoil is improved significantly. This paper aims to explore the effect of camber on the L/D ratio of an airfoil using the CFD method, thereby optimizing the airfoil design. A simulation would be performed for a series of airfoils that have the same shape parameters except for camber. The L/D ratio of these airfoils at different AOA would be calculated, and the results of these airfoils would be compared with each other, thereby determining which airfoil has the optimal L/D ratio.

2. Method

2.1. Airfoil design parameters

An airfoil is the cross-section profile of a wing. The design of an airfoil has a curved upper surface and a relatively flat lower surface, thus the air flowing over the airfoil travels faster than the air flowing below the airfoil. According to Bernoulli's principle, the airflow over the airfoil creates low pressure and the airflow below the airfoil creates high pressure, thereby resulting in a pressure difference between the upper and lower surfaces of the airfoil. The pressure difference gives the airfoil an upward lift force. The geometric shape of an airfoil is shown in Figure 1. An airfoil contains many important shape parameters such as maximum camber, maximum thickness, and positions in percent chord. All the parameters should be taken into account in airfoil design as each parameter would affect the performance of the airfoil. If the chord line coincides with the mean camber line, then the shape of the airfoil is symmetric [9].

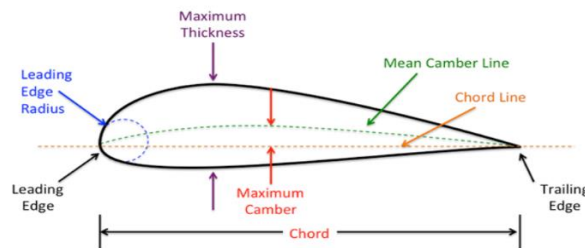


Figure 1. Geometric features of an airfoil.

2.2. NACA airfoil and airfoil selection

NACA is the abbreviation of National Advisory Committee for Aeronautics. In the late 1920s and early 1930s, NACA developed a series of airfoils and used a series of digits to represent the geometric features of each airfoil. The NACA airfoils contain 4-digit, 5-digit and modified 4-/5-digit airfoils. For NACA 4-digit airfoils, the first digit represents the maximum camber in the percentage of the chord, the second digit represents the position of the maximum camber, and the last two digits represent the maximum thickness in the percentage of the chord. NACA 2418, NACA 4418 and NACA 6418 airfoils are used in the CFD simulation. According to the four digits of these three airfoils, they have the same shape parameters except for camber, and NACA 6418 airfoil has the highest camber and NACA 2418 airfoil has the lowest camber.

2.3. COMSOL multiphysics 5.6

The simulation was conducted with a stationary solver using the software COMSOL Multiphysics 5.6. COMSOL is an engineering simulation software that simulates various engineering and physics problems with the finite element analysis method such as fluid, acoustic and mechanical. Researchers usually attempt various solutions to the problem required to obtain the expected simulation result when using this software [10].

2.4. Airfoil and fluid domain modelling

The contour of the airfoil is developed using Airfoil Tool as shown in Figure 2, and then it is imported into COMSOL to obtain the 2D model of the airfoil. The airfoil is placed in a fluid domain which represents a large wind tunnel as shown in Figure 3. Figure 3 also shows the boundary conditions of the fluid domain. The chord of the airfoil is 1 m, the fluid domain is 6 meters long and 4 meters high, the inlet is velocity based and has a velocity component of $U_{0x}=45$ m/s, $U_{0y}=0$ m/s, the outlet is pressure based and has a static pressure of 0 Pa, and the airfoil is defined as the no-slip wall. The airfoil is rotated for AOA from 0° to 20° at an interval of 2° during the simulation. In addition, the k-omega SST turbulence model is used for the simulation, and the working fluid is ideal air.

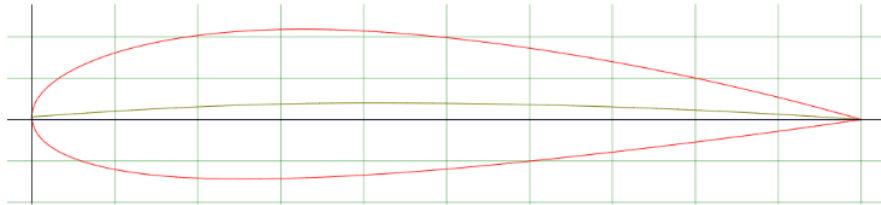


Figure 2. Airfoil contour (sample of NACA 2418).

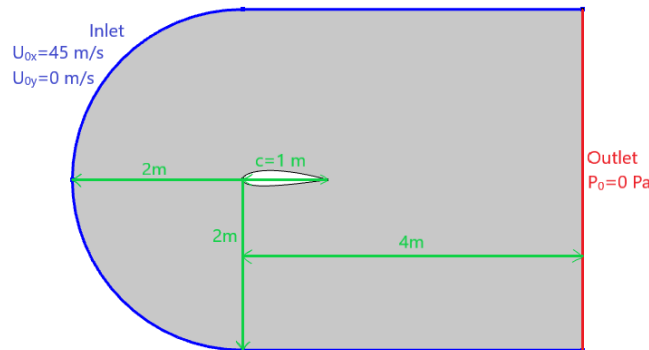


Figure 3. Fluid domain and boundary conditions (sample of NACA 2418).

2.5. Mesh generation

Solvers cannot solve the governing equation directly as the shape of the object is complex and irregular. Therefore, meshing is applied to the models in CFD simulation [11]. Meshing divides a complex object into many well-defined cells where the governing equation can be applied so that the solver can effectively perform the simulation of physical behavior. The quality of the mesh determines the accuracy of the simulation result directly. A fine mesh usually gives an accurate simulation result but requires a longer computation time, and a coarse mesh cannot ensure a very accurate result but the computational time can be saved. It can be seen from Figure 4 that unstructured mesh is applied to the model. The mesh is generated using physics-controlled with normal element size that comes with COMSOL. It can be seen from Figure 4 that the mesh is very fine around the airfoil but it is relatively coarse in other areas of the fluid domain, this is because the interest of the simulation is in the airfoil. In addition, inflation is also applied to the airfoil so that the velocity gradient near the airfoil can be accurately captured as shown in Figure 4.

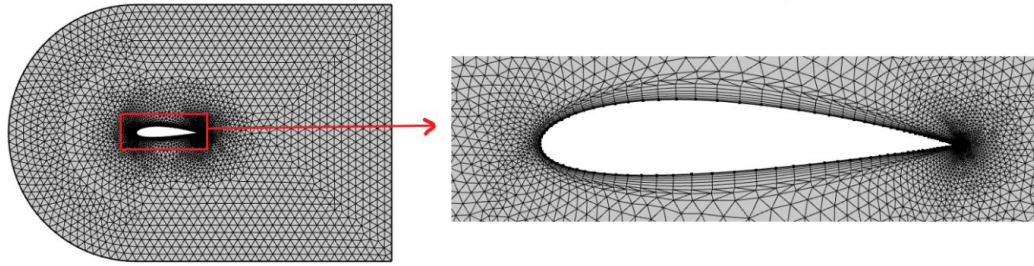


Figure 4. Mesh for the model (sample of NACA 2418).

2.6. Flow visualization

Flow visualization is to simulate the motion of the fluid, thereby presenting the flow field. The black lines represent the streamlines and are imagined. These streamlines describe the flow path of the fluid. Performing flow visualization helps CFD engineers to analyse, explore and understand their CFD results. In addition, the flow visualization shows the velocity distribution in the flow field using the velocity magnitude contour. Different colors in the velocity contour represent different flow velocities from the minimum to the maximum, and the velocity contour also presents the velocity distribution in the flow field. Therefore, it is easy to get to know the velocity at different locations in the flow field.

2.6.1. Flow field around NACA 2418. Figure 5 (a) shows the flow field around the NACA 2418 airfoil at the maximum L/D ratio. It can be seen that the airflow is closely attached to the airfoil and travels smoothly along the surface of the airfoil. Figure 5 (b) shows the flow field around the NACA 2418 airfoil under stall conditions. It can be seen that the NACA 2418 airfoil is stalled at 16° AOA, the airflow separates from the top surface of the airfoil, and vortices are created in the flow separation region after the separation point.

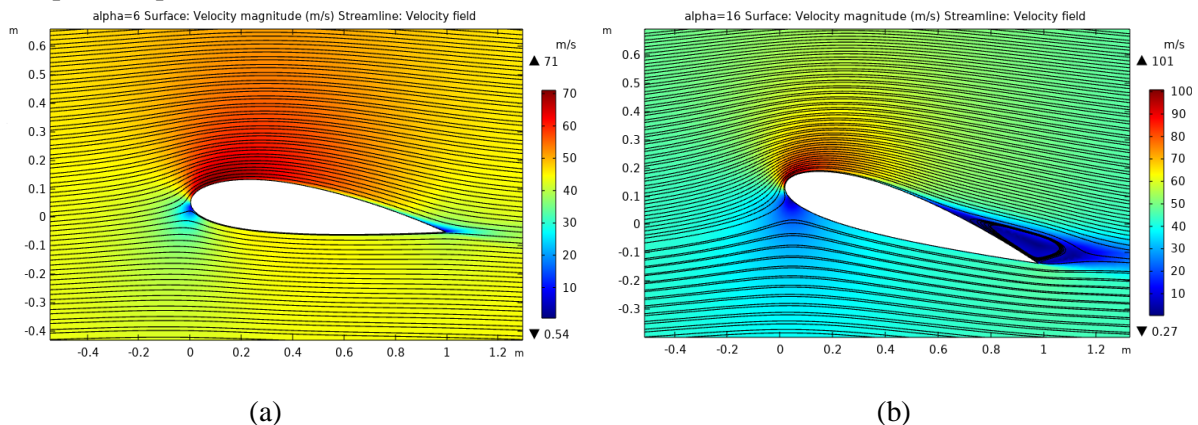


Figure 5. Flow field around NACA 2418 airfoil at (a). Maximum L/D ratio at 6° AOA, (b). Stall at 16° AOA.

2.6.2. Flow field around NACA 4418. Figure 6 (a) and Figure 6 (b) show the flow field around the NACA 4418 airfoil in the case of maximum L/D ratio and stall state respectively. It can be seen from Figure 6 (b) that NACA 4418 airfoil is stalled at the AOA of 18° and flow separation occurs in the upper surface of the airfoil. The velocity of the airflow above the airfoil is greater than that of airflow below the airfoil as shown in Figure 6 (a), which can be combined with Bernoulli's principle to explain why the lift force is produced.

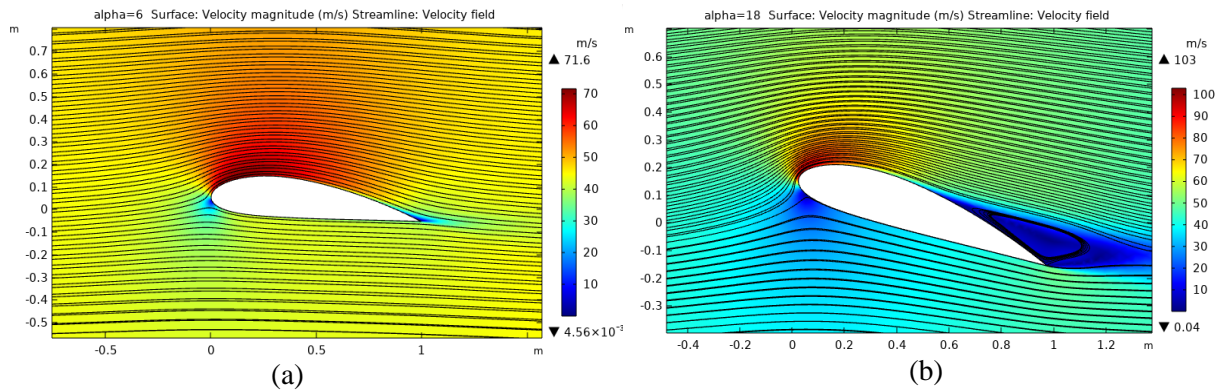


Figure 6. Flow field around NACA 4418 airfoil at (a). Maximum L/D ratio at 6° AOA, (b). Stall at 18° AOA.

2.6.3. *Flow field around NACA 6418.* Figure 7 (a) and Figure 7 (b) show the flow field around the NACA 6418 airfoil in the case of maximum L/D ratio and stall state respectively. It can be seen that the features of the flow field around the NACA 6418 airfoil are quite similar to both NACA 2418 and NACA 4418. NACA 6418 airfoil is also stalled at 18° AOA as shown in Figure 7 (b).

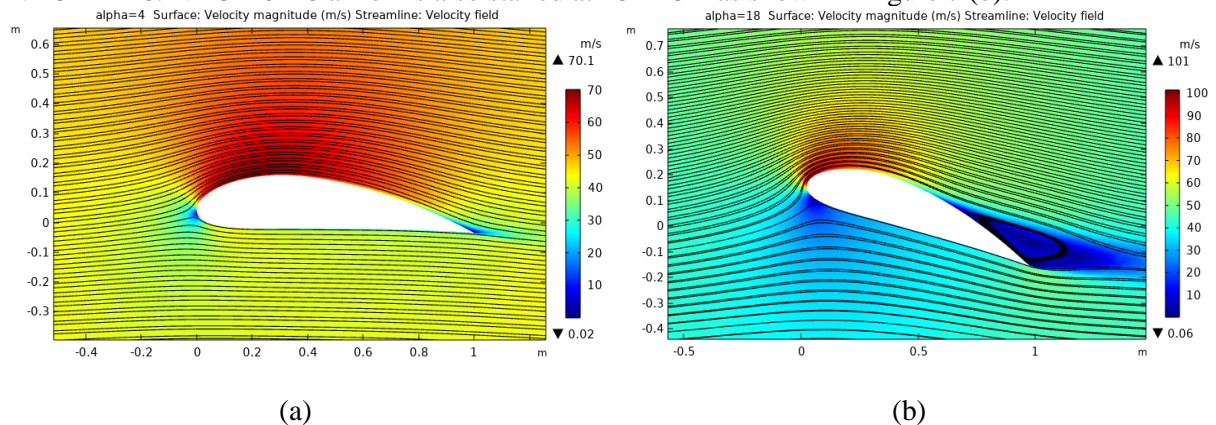


Figure 7. Flow field around NACA 6418 airfoil at (a). Maximum L/D ratio at 4° AOA, (b). Stall at 18° AOA.

2.7. *Experimental data from literature*

Jacobs, Ward and Pinkerton [12] systematically studied the aerodynamic characteristics of 78 different airfoils at a specific Reynolds number. The experimental data [12] of Jacobs, Ward and Pinkerton for NACA 2418, NACA 4418 and NACA 6418 is shown in Figure 8. Figure 8 (a) shows the experimental data for NACA 2418. It can be seen that the maximum L/D ratio is approximately 43.5 and occurs at the AOA of 4°. Figure 8 (b) shows that the maximum L/D ratio for NACA 4418 airfoil is approximately 45, occurring at the AOA of 2°. In addition, the value of the maximum L/D ratio for NACA 6618 airfoil is approximately 50 and is reached at the AOA of approximately 1° as shown in Figure 8 (c). The experimental data will be compared with the CFD results later.

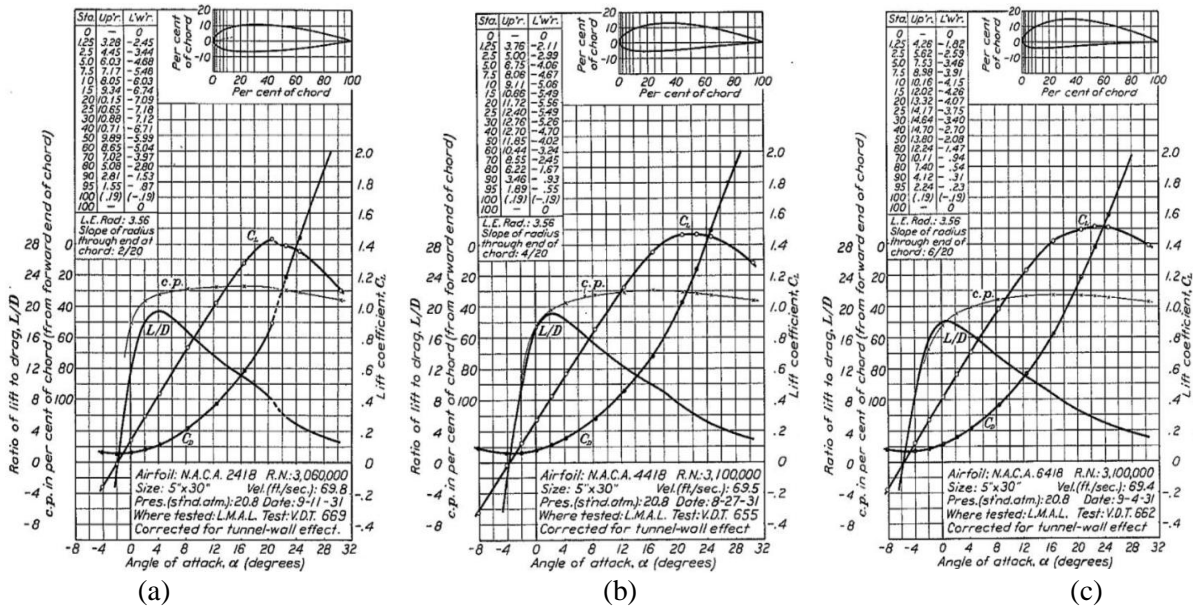


Figure 8. Experimental data for (a). NACA 2418, (b). NACA 4418 and (c). NACA 6418.

3. Result

3.1. CFD results of NACA 2418

Figure 9 illustrates the relationship between the L/D ratio and the AOA for NACA 2418 airfoil. The L/D ratio increases at the AOA from 0° to 6° and then decreases at the AOA from 6° to 20° . The maximum L/D ratio is 36.5373 and occurs at the AOA of 6° . Besides, NACA 2418 airfoil is stalled at 16° AOA as discussed before, and Figure 9 shows that the L/D ratio is 18.8564 at 16° AOA, which means the L/D ratio is 18.8564 when the airfoil is stalled.

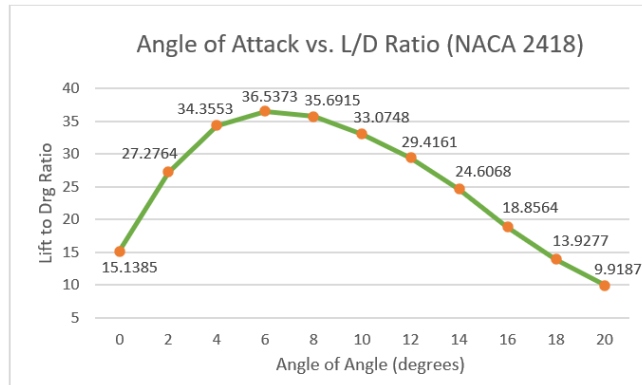


Figure 9. L/D ratio versus AOA for NACA 2418 airfoil.

3.2. CFD results of NACA 4418

Figure 10 shows the L/D ratio of NACA 4418 airfoil at different AOA. The L/D ratio increases at the AOA from 0° to 6° and reaches the peak value of 39.6551 at the AOA of 6° . After that, the L/D ratio starts to decrease till the AOA of 20° . In addition, the stall AOA of NACA 4418 airfoil is 18° as discussed before, and it can be seen from Figure 10 that NACA 4418 airfoil reaches the L/D ratio of 16.0125 at the stall AOA.

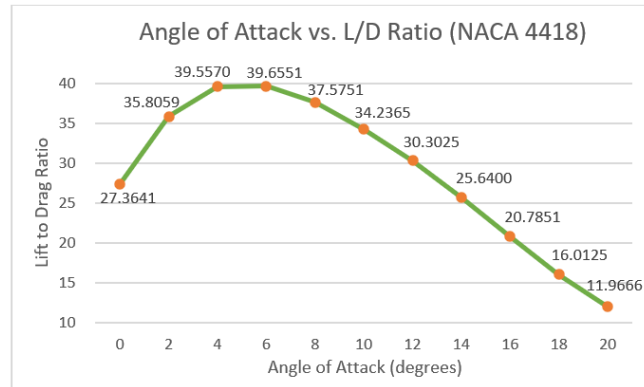


Figure 10. L/D ratio versus AOA for NACA 4418 airfoil.

3.3. CFD results of NACA 6418

As shown in Figure 11, the relationship between the L/D ratio and the AOA for NACA 6418 airfoil has a similar trend with NACA 2418 and NACA 4418. The maximum L/D ratio of NACA 6418 airfoil is 41.9536 and occurs at the AOA of 4°. After reaching the maximum, the L/D ratio starts to decrease till the AOA of 20°. The stall of the NACA 6418 airfoil occurs at 18° AOA, and the L/D ratio under stall is 17.528 as shown in Figure 11.

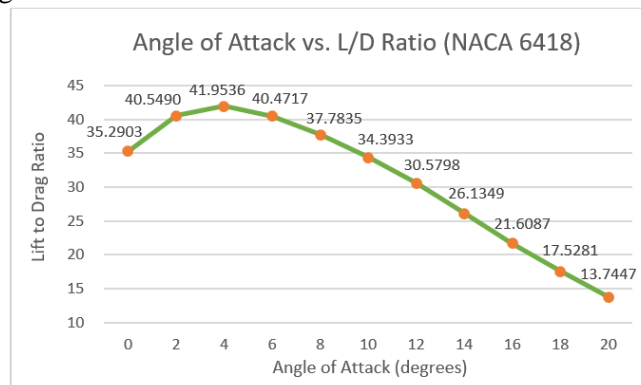


Figure 11. L/D ratio versus AOA for NACA 6418 airfoil.

4. Discussion

The results show that the L/D ratio of NACA 6418 is higher than that of NACA 4418 and NACA 2418 at each AOA, and the L/D ratio of NACA 4418 is higher than that of NACA 2418 at each AOA, in contrast, NACA 2418 shows the worst L/D ratio. In addition, the experimental data shown in Figure 8 also shows the same result. As mentioned before, NACA 6418 has the highest camber, secondly, it is NACA 4418, and NACA 2418 has the lowest camber. Therefore, NACA 6418 has the optimal L/D ratio and it can be concluded that the L/D ratio of an airfoil increases with the camber when the other shape parameters remain constant.

However, it can be seen that the numerical values of the simulation results are a little bit different from the experimental data shown in Figure 8. The errors may be caused by two reasons. One is that the experimental data is based on experiments, whereas the simulation results are based on CFD simulation, errors always exist between experiments and CFD. Another one is that the CFD simulation is performed at a different Reynolds number from the experiment. In order to improve the accuracy of the simulation, some methods like finer mesh, appropriate turbulent flow model and boundary condition can be applied to the simulation to decrease the errors.

5. Conclusion

In conclusion, this study conducted a CFD analysis for NACA 2418, NACA 4418 and NACA 6418 to optimize the airfoil design in terms of the camber of the airfoil. NACA 6418 has the optimal L/D ratio compared to NACA 4418 and NACA 2418 as NACA 6418 has the maximum camber, NACA 4418 has the higher L/D ratio than NACA 2418, and NACA 2418 has the worst L/D ratio as its camber is the lowest. Therefore, when designing an airfoil, a high camber could be applied to the airfoil to improve the L/D ratio of the airfoil. In addition, the L/D ratio will probably be affected by other factors such as the density of air, the wing aspect ratio and the ground effect, hence it is necessary to take these factors into account in further research.

References

- [1] Gudmundsson, S 2014, 'Performance-Cruise', General aviation aircraft design: applied method and procedures, Butterworth-Heinemann, Oxford, pp. 847-894.
- [2] Young, T & Hirst, M 2012, 'Revolutionary ideas about the future of air transport', Innovation on Aeronautics, Woodhead Publishing, Sawston, pp. 233-259.
- [3] Acarer, S 2020, 'Peak lift-to-drag ratio enhancement of the DU12W262 airfoil by passive flow control and its impact on the horizontal and vertical axis wind turbines', Energy, vol. 201, p. 117659.
- [4] Sogukpinar, H & Bozkurt, I 2015, 'Calculation of Optimum Angle of Attack to Determine Maximum Lift to Drag Ratio of NACA 632-215 Airfoil', Journal of Multidisciplinary Engineering Science and Technology, vol. 2, no. 5, pp. 1103-1208.
- [5] Hong, Z, Yu, T, Chen, G, Li, X & Hong, Y 2019, 'Simulation Analysis on the Blade Airfoil of Small Wind Turbine', Earth and Environmental Science, vol. 295 (2), p. 12079.
- [6] Haryanto, I, Utomo, M, Sinaga, N, Rosalia, C & Putra, A 2014, 'Optimization of Maximum Lift To Drag Ratio On Airfoil Design Based On Artificial Neural Network Utilizing Genetic Algorithm', Applied Mechanics and Materials, vol. 493, pp. 123-128.
- [7] Zhang, J, Guo, W, Zhang, P & J, H 2023, 'Optimizing Airfoil Aerodynamic Characteristics by Using Proposed CSA-KJ Method', Applied Sciences, vol. 13(2), p. 924.
- [8] He, Y, Agarwal, RK & Ganguli, R 2014, 'Shape Optimization of NREL S809 Airfoil for Wind Turbine Blades Using a Multiobjective Genetic Algorithm', International Journal of Aerospace Engineering, vol. 2014, p.1-13.
- [9] Houghton, EL, Carpenter, PW, Collicott, ST & Valentine, DT 2017, Aerodynamics for Engineering Students (Seventh Edition), 7th edn, Butterworth-Heinemann, Oxford.
- [10] Tulus, Khairani, C, Marpaung, TJ & Suriati 2019, 'Computational Analysis of Fluid Behaviour Around Airfoil with Navier-Stokes Equation', Journal of Physics: Conference Series, vol. 1376 (1), p.12003.
- [11] Cadence, 2023, The Importance of Meshing in CFD and Structural FEA, Cadence, viewed 20 April 2023, <<https://resources.system-analysis.cadence.com/blog/msa2022-the-importance-of-meshing-in-cfd-and-structural-fea>>.
- [12] Jacobs, E, Ward, K & Pinkerton, R 1933, The characteristics of 78 related airfoil sections from tests in the variable-density wind tunnel, the U.S. Federal Government, Washington.